ELSEVIER

PII: S0032-3861(97)00089-X

Polymer Vol. 38 No. 21, pp. 5275–5281, 1997

0032-3861/97/$17.00 + 0.00

Morphology of model three-component three-arm star-shaped copolymers

Shigeru Okamoto*, Hirokazu Hasegawa and Takeji Hashimoto†
Department of Polymer Chemistry, Graduate School of Engineering, Kyoto University, Kyoto 606-01, Japan

and Teruo Fujimoto‡, Hongmin Zhang§, Takeo Kazama, Atsushi Takano and Yoshinobu Isono
Department of Chemistry, Nagaoka University of Technology, Nagaoka, Niigata 940-21, Japan
(Received 18 December 1996; accepted 10 January 1997)

The microdomain structure of a model three-component, three-arm, star-shaped copolymer consisting of polystyrene (PS), poly(dimethylsiloxane) (PDMS) and poly(tert-butyl methacrylate) (PTBMA), each of them having nearly the same weight fraction, was investigated by means of differential scanning calorimetry (d.s.c.), transmission electron microscopy (TEM) and small-angle X-ray scattering (SAXS). D.s.c. results exhibiting the glass transition of PS and PTBMA and the crystallization and melting of PDMS strongly suggest the microphase separation of the three components into three microdomains. The microdomain structure is considered to be extremely complicated because the chemical junction points of the three constituent polymers must be confined on the lines where three kinds of interfaces meet. TEM and SAXS results strongly support the existence of a very regular microdomain structure with three-fold symmetry. Each of the three components possibly forms a three-dimensionally continuous network domain resulting in an ordered tricontinuous microdomain structure. © 1997 Elsevier Science Ltd.

(Keywords: block copolymer; star copolymer; microdomain)

INTRODUCTION

There is no doubt about the importance of multi-component multiphase polymer systems (or 'polymer alloys') in terms of both academic interest and practical use. Graft and block copolymers were a new class of polymers belonging to such systems and they had a great impact on the world when they were first introduced. The copolymers we introduce in this and the previous paper[1], ABC three-arm star-shaped copolymers (hereafter abbreviated as 'ABC stars'), are another new class of polymers. We believe that they will develop a completely different physical situation and have a great impact again. In the previous paper we reported the synthesis techniques of the model ABC stars[1] and in this paper we report the preliminary results of our study on their morphology.

The synthesis and the morphology of the three-arm star copolymers consisting of polystyrene (PS), polyisoprene and polybutadiene arms named 'miktoarm' (mixed-arm) copolymers were reported by Hadjichristidis and his co-workers[2,3]. However, their miktoarm copolymer and our ABC stars are essentially different as described below. Our copolymers, ABC stars, are the asymmetric star-shaped copolymers comprising three arms, i.e. PS, poly(dimethylsiloxane) (PDMS) and poly(tert-butyl methacrylate) (PTBMA), having completely different chemical natures and hence forming three different microphases composed of each constituent polymer. On the other hand, the miktoarm copolymers consist of PS, polyisoprene and polybutadiene arms. Since the latter two are miscible, the copolymers can form only two different microphases. Therefore, they are considered as 'ABB' stars' according to our terminology. The molecular architectures of ABC stars and ABB' stars are similar, but their difference is not trivial. The microphase separation of the latter may be similar to that of AB_2 graft copolymers (A polymer grafted on to B polymer)[3,4]. However, the former is considered as a new type of polymeric material and might exhibit entirely new morphology and physical properties different from existing polymeric materials such as ordinary graft copolymers and linear block copolymers[5–7]. It will also bring about interesting problems in polymer physics. The reason why ABC stars are so different and important is discussed below.

It is expected that the characteristic molecular architecture of ABC stars with the three different arms connected at a single point plays an important role and this problem must be investigated both experimentally and theoretically. If the constituent polymers of the ABC stars are immiscible with each other, they undergo microphase separation to form three different phases, but the way they form microdomain structures should

* Present address: Department of Materials Science and Engineering, Nagoya Institute of Technology, Gokiso-cho, Showa-ku, Nagoya 466, Japan
† To whom correspondence should be addressed
‡ Deceased
§ Present address: 11 Beijing University of Technology, Beijing 100029, P. R. China

be very different from that of AB diblock or linear ABC triblock copolymers, as schematically illustrated in *Figure 1*. In the case of AB diblock copolymers in the strong segregation regime, the chemical junction points between A and B block chains are always confined on the *interfaces* (or in the narrow interfacial regions) between A and B microdomains regardless of the microdomain morphology (*Figure 1a*). The situation is the same for linear ABC triblock copolymers (*Figure 1b*) although a greater variety of microdomain morphologies are possible for linear ABC triblock copolymers[8–14]. However, the situation is quite different for ABC stars. When the three components form their own microdomains, the chemical junction points of the three arms of ABC stars must be confined not only on the interfaces but also on the *lines* where three different microdomain interfaces, i.e. the interfaces between A and B, between B and C and between C and A microdomains, intersect each other (*Figure 1c*). This topological constraint will restrict the microdomain morphology of ABC stars to very special ones. If the volume fractions of the three microdomains are all equal, two kinds of regular structure are intuitively derived: one consists of hexagonal columns of each microdomain and the other consists of lozenge-shaped columns of each microdomain, as illustrated in *Figures 2a* and *2b*, respectively. However, these models are strictly limited to the ABC stars having exactly the same volume fractions for the three components. What will be the microdomain structure if the volume fractions of the three components are not exactly the same? It is not easy to answer this question because it is not only a problem of polymer science but also a new problem in geometry. Therefore, we think it is worthwhile to show the results of our observation in this paper, although the structure is not yet clarified.

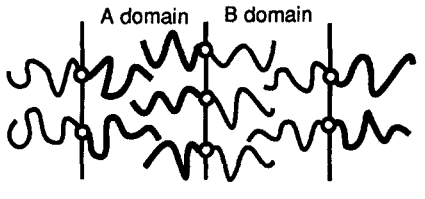

(a) AB diblock copolymer

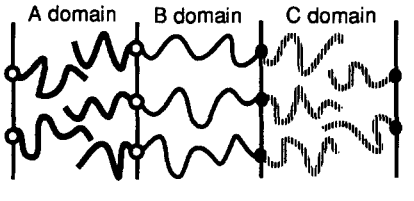

(b) ABC linear triblock copolymer

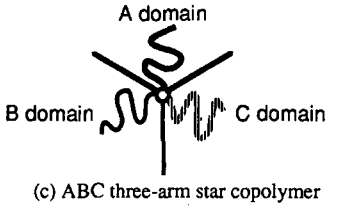

(c) ABC three-arm star copolymer

Figure 1 Schematic illustrations of the arrangement of copolymer chains. (a) AB diblock copolymer: the chemical junction points are confined on the interface; (b) linear ABC triblock copolymer: the chemical junction points are confined on the interfaces; (c) ABC star: the chemical junction points are confined on a line

If the segregation power between B and C components of ABC stars decreases at high temperatures, B and C might mix to form a single phase resulting in the ordinary two-phase microdomain structures as illustrated in *Figure 3a*. In such cases, the ABC stars will behave similarly to AB_2 graft copolymers, and the chemical junction points are located in the interfacial region between the A microdomain and the microdomain composed of the mixture of B and C. Such an example was reported for the miktoarm copolymers of ABB′ type[3,15,16]. Change in the temperature may cause further phase separation between B and C, resulting in a microdomain structure of three different phases. Depending on the temperature dependence of the pairwise interaction among the three components, transitions from the structure shown in *Figure 3a* to that in *Figures 3b* and *3c* might take place when the temperature changes.

The topologically constrained ABC stars are anticipated to have unique features in the phase transitions as well. The order–disorder transition and order–order transitions must be intuitively different from those of various linear block copolymers, which have been

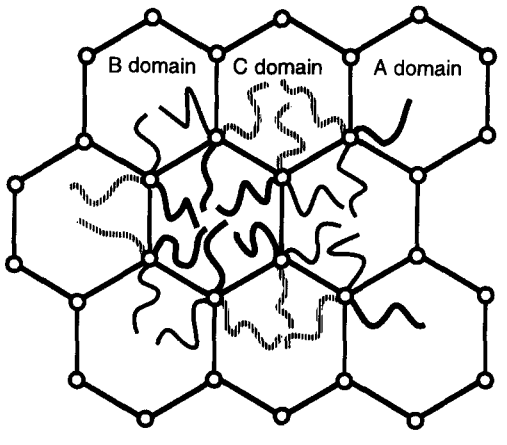

(a)

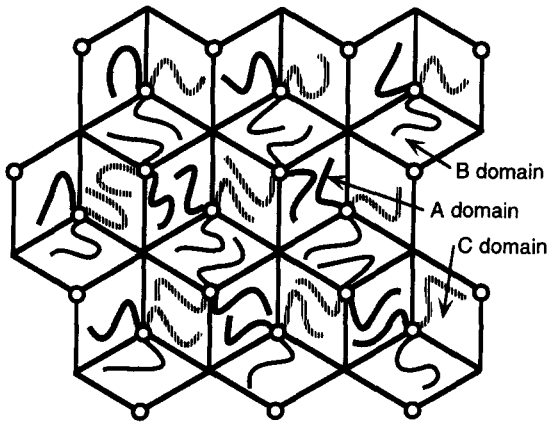

(b)

Figure 2 Possible microdomain structure models for the particular ABC star having equal volume fractions of the three components: (a) each microdomain consists of a hexagonal column; (b) each microdomain consists of a lozenge-shaped column. The chemical junctions are located on the lines normal to the paper as marked by circles. The circles form the same two-dimensional hexagonal array for both cases

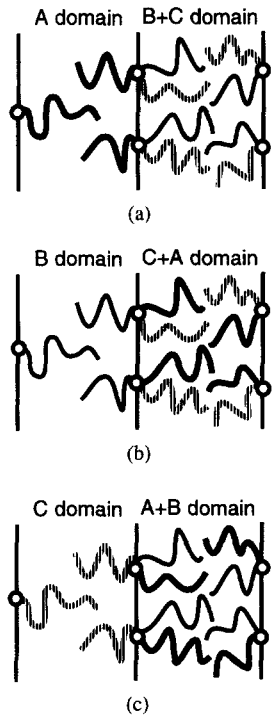

Figure 3 Schematic illustrations of the arrangement of ABC star chains. (a) B and C components are mixed to form a single phase: the chemical junctions are confined in the interfacial region; (b) C and A components are mixed; (c) A and B components are mixed

Table 1 Characterization of three-component, three-arm star-shaped copolymers

Sample code	$10^{-4}M_n$ (total)	PS (wt%)	PDMS (wt%)	PTBMA (wt%)
S-ZH(222)	5.9	27	37	36
S-ZH(333)	10.0	34	35	31
S-ZH(444)	13.5	36	26	38

extensively studied up to now. Thus, we propose the ABC stars as a truly new class of multicomponent polymers and as a new generation in a series of block and graft copolymers which have been developed so far.

EXPERIMENTAL

Samples

Three model ABC star copolymers, S-ZH(222), S-ZH(333) and S-ZH(444), the synthesis and the purification of which were reported in our first paper[1], were investigated in this study. The characterization of these samples are listed in *Table 1*. The three arms of the copolymers consist of PS, PDMS and PTBMA, each of them having nearly the same weight fraction (but not exactly the same). Each of the three digits in the parentheses of the sample codes gives the approximate molecular weight of each component in units of 10 kg mol^{-1}. Besides the star-shaped copolymers, some of the corresponding diblock copolymers, i.e. polystyrene-*block*-poly(dimethylsiloxane) (PS–PDMS) and polystyrene-*block*-poly(tert-butyl methacrylate) (PS–PTBMA) were also prepared separately or obtained as aliquots in the course of synthesis of the star-shaped copolymers. These diblock copolymers were used as the reference material in thermal analysis. All the samples were cast at room temperature from solutions in toluene, which is a good solvent for all three components. The cast films were further dried under vacuum for one to two days at room temperature and used for the experiments.

Thermal analyses

Measurements by thermogravimetric–differential thermal analysis (t.g.-d.t.a.) were performed on the star-shaped copolymers and the diblock copolymers in the heating process from 25 to 450°C at a heating rate of 20°C min^{-1} with a Rigaku TAS-200 thermal analysis system. Differential scanning calorimetry (d.s.c.) was performed on those samples with a Perkin-Elmer DSC 7 calorimeter. The samples were first heated to 200°C at a heating rate of 20°C min^{-1}, held at 200°C for 3 min, and cooled to 50°C at a cooling rate of −320°C min^{-1}. The d.s.c. data were collected for a second heating cycle from 50 to 200°C at a heating rate of 20°C min^{-1}. For the low temperature measurements, the samples were cooled down to −130°C and the d.s.c. data were collected for the heating cycle from −130 to 0°C at a heating rate of 20°C min^{-1}. The temperature was calibrated using the melting peaks of indium and zinc.

Transmission electron microscopy (TEM)

The as-cast film specimens were embedded in epoxy resin without prestaining. The samples were then subjected to ultramicrotoming into ultrathin sections of *ca* 50 nm thick at room temperature with an LKB Ultrotome type 4802A ultramicrotome using glass knives. The ultrathin sections without any staining served for the TEM investigation with a Hitachi H-600S transmission electron microscope operated at 100 kV.

Small-angle X-ray scattering (SAXS)

SAXS profiles of the as-cast film specimens were measured with a Rigaku rotating anode X-ray generator of 12 kW with a monochromatized CuK_α line and a 1.5 m X-ray camera with a one-dimensional position sensitive proportional counter[17]. The profiles were obtained for the edge (the incident X-ray beam is parallel to the film surfaces and the scattering intensity distribution normal to the film surface is measured) and through configurations (the incident X-ray beam is perpendicular to the film surfaces and the scattering intensity distribution parallel to the film surface is measured), corrected for absorption, background scattering arising from the thermal diffuse scattering, and slit-width and slit-height smearing effects[18], and converted into the absolute unit (electron^2 nm^{-3})[19].

RESULTS AND DISCUSSION

Thermal analyses

The t.g. curves show the change in weight of the samples and thus give information about their thermal stability. For S-ZH(222) the weight started to decrease gradually from *ca* 200°C and an abrupt drop was observed at *ca* 260°C, which coincides with a sharp exothermic peak in the d.t.a. curve. This abrupt change in weight is attributed to the decomposition of PTBMA, as the same behaviour was observed for the aliquot PS–PTBMA diblock copolymer. The observations of weight

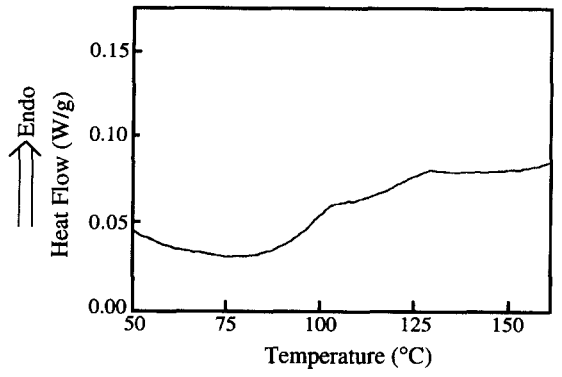

Figure 4 D.s.c. curves for the second heating process of S-ZH(222) toluene-cast film for the higher temperature region (50–160°C). The heating rate is 20 K min^{-1}

loss and exothermic peaks at *ca.* 200°C due to anhydride formation on thermal treatment of PTBMA homopolymers have been reported[20]. The thermal stability decreases with increasing molecular weight of the ABC stars. For S-ZH(444) the weight loss became significant above *ca* 130°C. Thus, the annealing of S-ZH(444) may cause an undesirable change in the chemical structure of the sample, and the TEM observation was limited to the as-cast film.

Figure 4 shows the d.s.c. curve for S-ZH(222) for the higher temperature region. Two endothermic shifts were observed in the thermogram. They are considered as the glass transition temperatures (T_g) of the PS and PTBMA components. The T_g (midpoint) evaluated from the d.s.c. curve was 96 and 121°C. The former is in good agreement with the literature value of T_g for PS homopolymer (100°C) and the latter with that for atactic PTBMA homopolymer (118°C)[21]. This suggests that the microdomains giving rise to these T_g are composed of almost pure PS and PTBMA components, respectively. If the PDMS component had been mixed with either the PS or PTBMA component, as shown in *Figure 3*, the T_g of the microdomain composed of PS or PTBMA mixed with PDMS should have been moved to a temperature significantly lower than the T_g of pure PS or PTBMA, e.g. at −77 or −62°C, respectively, estimated by using −127°C for the T_g of pure PDMS[2] and the Fox equation[22]:

$$T_g^{-1} = w_1 T_{g1}^{-1} + w_2 T_{g2}^{-1} \quad (1)$$

where w_i is the weight fraction of component i ($i = 1$ or 2) in the microdomain, and T_{gi}^{-1} is the T_g of pure component i.

The aliquot PS–PTBMA diblock copolymers exhibited d.s.c. curves similar to that in *Figure 4*, exhibiting two T_g relevant to the PS and PTBMA microphases, while the PS–PDMS diblock copolymers showed only one T_g relevant to the PS microphase in the d.s.c. curves measured in the temperature range 50–200°C.

The existence of PDMS microdomains in the ABC star copolymer is further confirmed by the d.s.c. measurements of S-ZH(222) (*Figure 5b*) and the corresponding PS-PDMS diblock copolymer (*Figure 5a*) for the lower temperature region. In *Figure 5a* for the diblock copolymer an exothermic peak at −96°C and two endothermic peaks at −47 and −38°C were observed. The exothermic peak corresponds to the crystallization of PDMS component and the two endothermic peaks

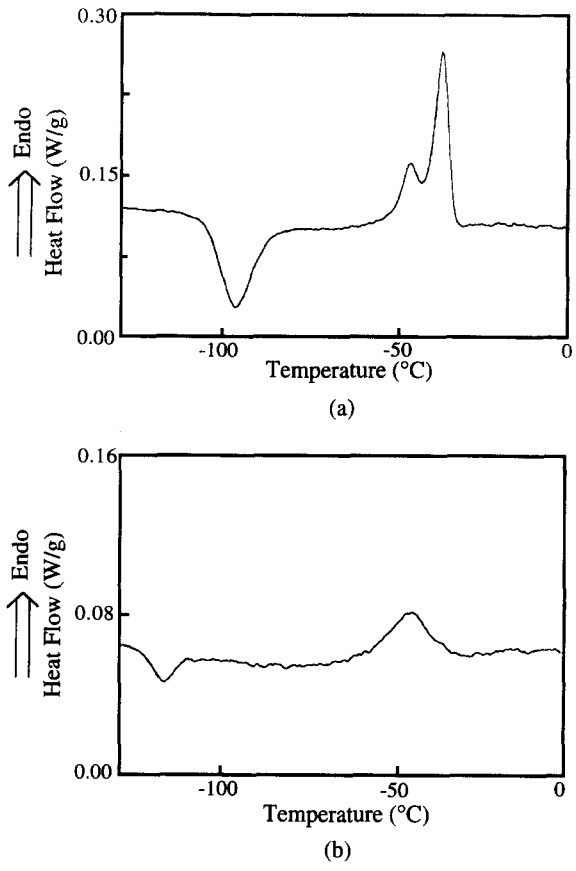

Figure 5 D.s.c. curves for the heating process of (a) PS–PDMS block copolymer and (b) S-ZH(222) toluene-cast films for the lower temperature region (−120 to 0°C). The heating rate is 20 K min^{-1}

correspond to the melting of the PDMS crystals crystallized probably during the cooling and heating processes. This observation is in good agreement with that reported for the microphase-separated PS–PDMS block copolymers by Feng *et al.*[23]. Their measurement went down to −150°C, which was 20°C below our lower limit, and they observed the glass transition of the PDMS component having a similar molecular weight (M_n = 19 300) as ours at −125°C. Thus, an observation of PDMS crystallization in a PS–PDMS block copolymer is a strong indication of its microphase separation.

Figure 5b for S-ZH(222) clearly shows the exothermic peak of PDMS crystallization at *ca*-115°C and the endothermic peak of the melting of the PDMS crystals at *ca* −45°C. Therefore, the PDMS component in S-ZH(222) must be also forming its own microdomains independently. If the PDMS component of S-ZH(222) were mixed with one of the other components, PS or PTBMA, the T_g of the mixed phase should be much higher than −115°C [−77°C for the PDMS/PS mixed phase and −62°C for the PDMS/PTBMA mixed phase, according to the calculation with equation (1)] and PDMS would not crystallize at −115°C. The existence of a pure PDMS microphase is also supported by the absence of any T_g in the temperature range between −130 and 0°C. It should be noted that the crystallinity of the PDMS component in S-ZH(222) is much smaller than that in the corresponding PS–PDMS block copolymer, judged by the area of their melting peaks. This suggests that the PDMS chains in the microdomains of S-ZH(222) are more hindered from crystallization than those in the PS–PDMS block copolymer.

The d.s.c. results imply that all three components are microphase separated and forming their own microdomains in S-ZH(222), having the smallest molecular weight among the three ABC stars. Since the segregation power increases with increasing degree of polymerization, it is reasonable to conclude that the three components, PS, PTBMA and PDMS are microphase separated also in the other two ABC stars, S-ZH(333) and S-ZH(444).

TEM observation

TEM observation was performed on the ultrathin sections of the as-cast films without staining because Si atoms in the PDMS component give a good contrast[23]. *Figure 6* shows the typical images obtained from S-ZH(444) for (a) low and (b) high magnification. Since the only element giving rise to the dark contrast in the images is Si atoms, the darkness in different regions reflects the content of PDMS segments in the thickness direction of the ultrathin section. The two-dimensional array of dark triangular patterns exhibits a three-fold symmetry (b). The size of the dark triangles changes from one region (e.g. the region marked 'X') to another (marked 'Y') in (a) although the orientation and the spacing (*ca* 30 nm) of the periodic structure remain almost constant. This suggests that the regions X and Y have the same microdomain structure belonging to a single grain (the region where the microdomain structure is coherent), but sliced at different positions: the plane normal to the three-fold axis in the microdomain structure is slightly tilted with respect to the ultrathin section, and that the structures at different levels along the three-fold axis are seen as triangles with different sizes (note that the section thickness, *ca* 50 nm, is slightly larger than the structural periodicity). This implies that the microdomain structure has a periodicity along the three-fold axis because if it were composed of a two-dimensional array of three kinds of columnar microdomains, as illustrated in *Figure 2*, the pattern should appear the same regardless of the levels of the slices. This implication is more clearly seen in the bottom of (a) (the region marked 'Z') where another grain composed of the same microdomain structure with different orientation from that of regions X and Y is observed.

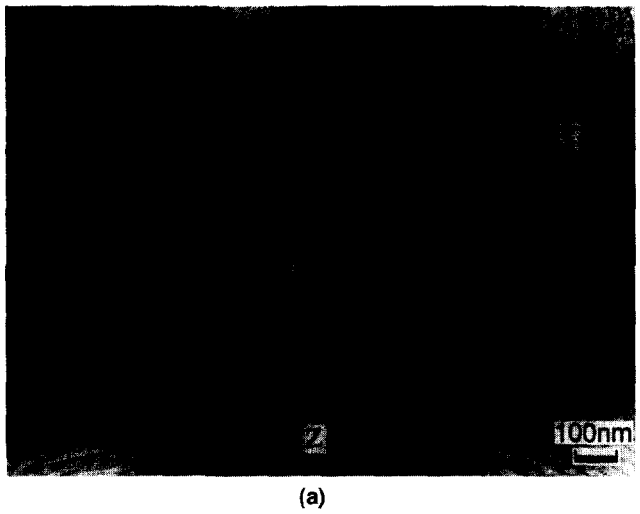

(a)

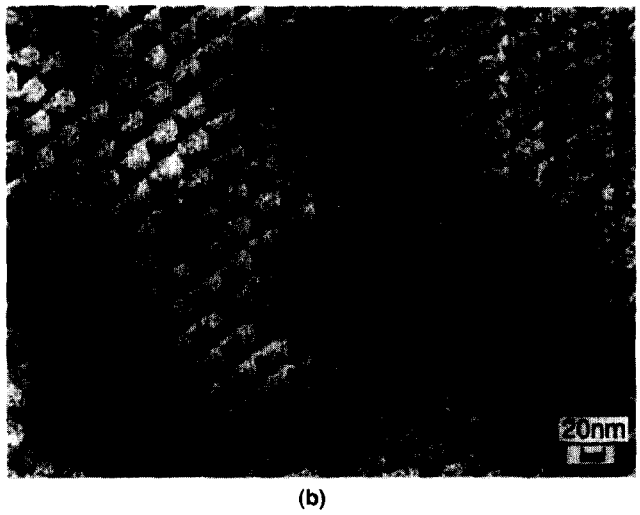

(b)

Figure 6 TEM micrographs obtained from an unstained ultrathin section of S-ZH(444) toluene-cast film: (a) low magnification; (b) high magnification

The appearance of the image in region Z is quite different from the region X or Y, but the microdomain structure itself is considered to be the same. It appears so different because the three-fold axis of this grain is significantly tilted with respect to the section normal. A layer-like (one-dimensional) periodicity (*ca* 50 nm), which is larger than 30 nm, is observed. Between the parallel dark lines dark triangles slightly elongated in the direction parallel to the dark lines are seen. Thus, the microdomain structure, which is periodic also along the three-fold axis, seems to be a complicated structure. The dark PDMS microphase is seen to be continuous in three dimensions as no single area is observed without greyish contrast.

Besides these patterns a variety of patterns were observed in different areas of the same or different sections. Nevertheless, those patterns are considered to originate from a single structure, i.e. they are different cross-sections of the same structure and just reflect the complexity of the structure. It may be understood from an example shown in *Figure 7*. Parts (a) and (b) are the TEM images obtained from the same area of an ultrathin section (*ca* 50 nm thick) of S-ZH(444), but in (b) the section is tilted by 25° in the microscope around the axis indicated by a broken white line. The patterns in the two micrographs appear to be quite different. The dark triangular patterns become more clear in (b).

To summarize, neither of the two simple models as shown in *Figure 2* can explain the TEM observations. The dark PDMS microdomain seems to be continuous in three dimensions. Therefore, it is natural to consider that the microdomains of PS and PTBMS, both appearing bright, are also continuous in three dimensions because the volume fraction of PDMS is less than 1/3. Although the PS and PTBMA microdomains are not distinguishable, it is reasonable to consider that both phases are continuous in three dimensions because their volume fractions are almost the same. Thus, a complicated but regular microdomain structure consisting of three continuous networks of different components is suggested for S-ZH(444).

S-ZH(222) seems to have a similar structure to S-ZH(444). However, the TEM micrographs are less clear because of the smaller microdomain size for the smaller molecular weight and because of the overlapping of the structure within the ultrathin sections.

SAXS

Figure 8 shows the SAXS profiles obtained for the

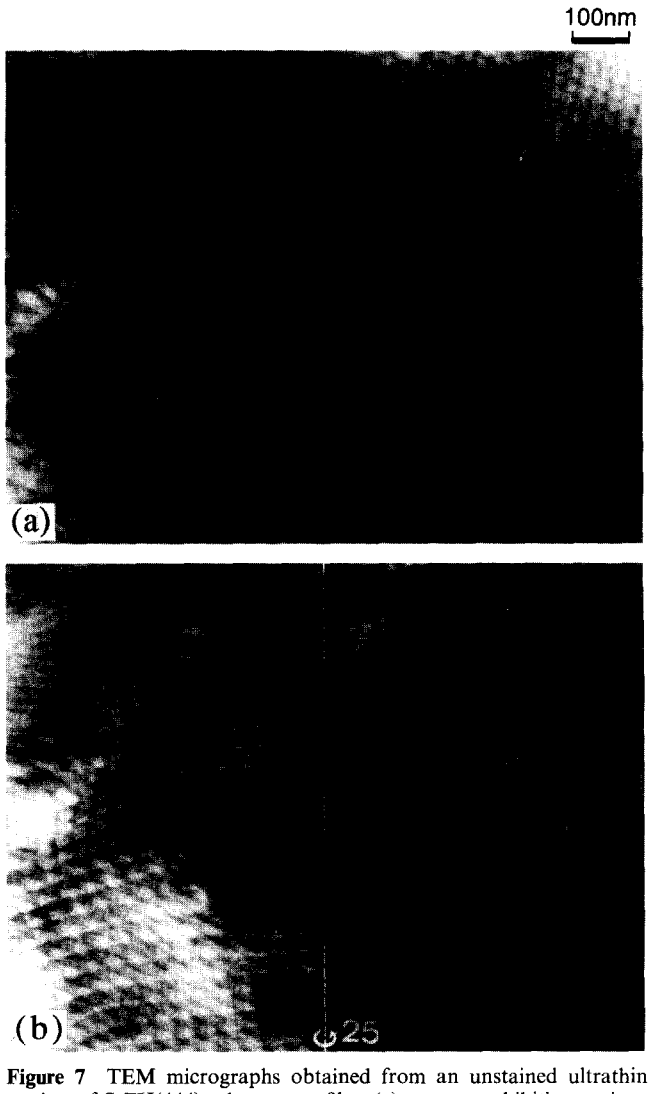

Figure 7 TEM micrographs obtained from an unstained ultrathin section of S-ZH(444) toluene-cast film: (a) an area exhibiting various patterns; (b) the same area as (a), but the section was tilted by 25° about the axis indicated by the white broken line

as-cast film of S-ZH(444) with two configurations, edge (triangles) and through (circles). The logarithm of the absolute intensity is plotted against the magnitude of the scattering vector: q $(= (4\pi/\lambda)\sin(\theta/2)$; θ: scattering angle, λ: wavelength). The difference between the two profiles can be attributed to the non-equilibrium effect set in the film specimen during the casting process. The structural relaxation parallel to the film surface was hindered by the interaction between the film and the substrate, resulting in a smaller spacing for the edge profile than the through profile. When the abscissa is normalized by q^*, the q value at the first-order peak, the edge and through profiles can be superimposed on top of each other as shown in the insertion of *Figure 8*.

The scattering profiles of S-ZH(444) exhibit multiple scattering peaks at q positions in the ratio of 1, $3^{1/2}$ and $7^{1/2}$. This strongly supports the existence of a very regular structure with three-fold symmetry as observed in the TEM images. The Bragg spacings evaluated from the first-order scattering peaks are 47 and 36 nm for the through and edge profiles, respectively. The latter is in good agreement with 30 nm, the spacing observed by TEM, which is reasonable because the ultrathin section is cut perpendicularly to the film surface and the TEM images correspond to the edge profile. Further analysis of the SAXS profiles will be performed when a possible model for the structure is evolved.

CONCLUSION

Three-component, three-arm star-shaped copolymers consisting of PS, PDMS and PTBMA, each of them having nearly the same weight fraction, were investigated by means of d.s.c., TEM and SAXS. The d.s.c. results exhibiting the glass transition of PS and PTBMA and the crystallization and melting of PDMS strongly suggest the microphase separation of the three components into three microdomains. TEM and SAXS results strongly support the existence of a very regular microdomain

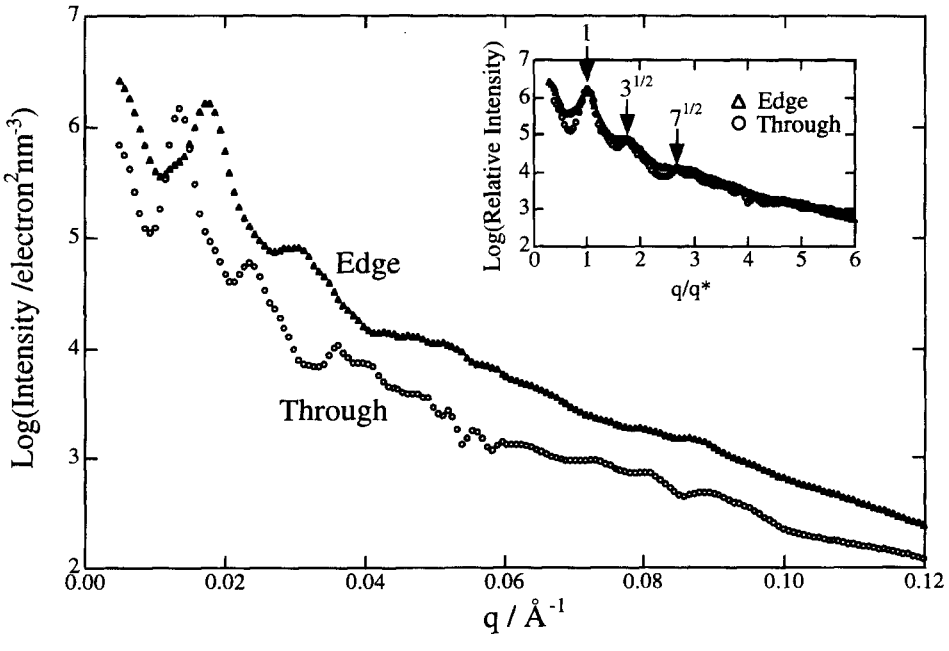

Figure 8 SAXS profiles for edge (open triangle) and through configurations (open circle) obtained from S-ZH(444) toluene-cast film. The insert shows the normalized profiles with the abscissa q/q^*

structure with a three-fold symmetry. Each of the three components possibly forms a three-dimensionally continuous network domain, resulting in an ordered tricontinuous microdomain structure.

ACKNOWLEDGEMENTS

The authors are grateful to Mr Y. Shuto, Daicel Chemical Industries, Ltd, for the d.s.c. and t.g.–d.t.a. measurements. This work was supported in part by a Grant-in-Aid for Scientific Research in Priority Areas for H.H. (08246229) and for Y.I. (08231231) from the Ministry of Education, Science, Sports and Culture, Japan.

REFERENCES

1. Fujimoto, T., Zhang, H., Kazama, T., Isono, Y., Hasegawa, H. and Hashimoto, T., *Polymer*, 1992, **33**, 2208.
2. Iatrou, H. and Hadjichristidis, N., *Macromolecules*, 1992, **25**, 4649.
3. Hadjichristidis, N., Iatrou, H., Behal, S. K., Chludzinski, J. J., Disko, M. M., Garner, R. T., Liang, K. S., Lohse, D. J. and Milner, S. T., *Macromolecules*, 1993, **26**, 5812.
4. Pochan, D. J., Gido, S. P., Pispas, S., Mays, J. W., Ryan, A. J., Fairclough, P., Hamley, I. W. and Terril, N., *Macromolecules*, 1996, **29**, 5091.
5. Molau, G. E., in *Block Polymers*, ed. S. L. Aggarwal. Plenum Press, New York, 1970, p. 79.
6. Hasegawa, H., Tanaka, H., Yamasaki, K. and Hashimoto, T., *Macromolecules*, 1987, **20**, 1651.
7. Bates, F. S. and Fredrickson, G. H., *Annu. Rev. Phys. Chem.*, 1990, **41**, 525.
8. Riess, G., Schlienger, M. and Marti, S., *J. Macromol. Sci., Polym. Phys. Ed.*, 1980, **17**, 355.
9. Arai, K., Kotaka, T., Kitano, Y. and Yoshimura, K., *Macromolecules*, 1980, **13**, 1670.
10. Shibayama, M., Hasegawa, H., Hashimoto, T. and Kawai, H., *Macromolecules*, 1982, **15**, 274.
11. Mogi, Y., Kotsuji, H., Kaneko, Y., Mori, K., Matsushita, Y. and Noda, I., *Macromolecules*, 1992, **25**, 5408.
12. Gido, S. P., Schwark, D. W., Thomas, E. L. and Goncalves, M. C., *Macromolecules*, 1993, **26**, 2636.
13. Stadler, R., Auschra, C., Beckmann, J., Krappe, U., Voigt-Martin, I. and Leibler, L., *Macromolecules*, 1995, **28**, 3080.
14. Zheng, W. and Wang, Z.-G., *Macromolecules*, 1995, **28**, 7215.
15. Floudas, G., Hadjichristidis, N., Iatrou, H., Pakula, T. and Fischer, E. W., *Macromolecules*, 1994, **27**, 7735.
16. Floudas, G., Hadjichristidis, N., Iatrou, H. and Pakula, T., *Macromolecules*, 1996, **29**, 3139.
17. Hashimoto, T., Suehiro, S., Shibayama, M., Saijo, K. and Kawai, H., *Polym. J.*, 1981, **13**, 501.
18. Fujimura, M., Hashimoto, T. and Kawai, H., *Mem. Fac. Eng., Kyoto Univ.*, 1981, **43**, 224.
19. Hendricks, R. W., *J. Appl. Crystallogr.*, 1972, **5**, 315.
20. Matsuzaki, K., Okamoto, T., Ishida, A. and Sobue, H., *J. Polym. Sci., Part A*, 1964, **2**, 1105.
21. Brandrup, J. and Immergut, E. H., *Polymer Handbook*, 3rd edn. John Wiley, New York, 1989, p. VI/218.
22. Fox, T. G., *Bull. Am. Phys. Soc.*, 1956, **1**, 123.
23. Feng, D., Wilkes, G. L. and Crivello, J. V., *Polymer*, 1989, **30**, 1800.